Journal of Controlled Release 366 (2024) 494–504

Contents lists available at ScienceDirect

Journal of Controlled Release

journal homepage: www.elsevier.com/locate/jconrel

Photo-controllable drug releasing bulk polyacrylic intraocular lens material for safer posterior capsular opacification prevention

Yulin Hu, Jiahao Wang, Yueze Hong, Yuemei Han, Lin Liang, Yuexin Yang, Zhihui Wu, Quankui Lin *

National Engineering Research Center of Ophthalmology and Optometry, School of Biomedical Engineering, School of Ophthalmology and Optometry, Eye Hospital, Wenzhou Medical University, Wenzhou 325027, China

ARTICLE INFO

Keywords:
Intraocular lens
5-fluorouracil
Photo-controllable drug release
Posterior capsular opacification
Bulk materials design

ABSTRACT

Posterior capsular opacification (PCO) is the most common complication that occurs after intraocular lens (IOL) implantation in cataract therapy. In recent years, IOLs have been developed as drug delivery platforms, but concerns over the safety of uncontrolled proliferative drug release have arisen. Therefore, a controlled drug release strategy is needed for safer PCO prevention. In this study, a new monomer contained coumarin group was introduced in material preparation, and poly(ethylene glycol phenyl ether methacrylate-*co*-2-(2-ethoxyethoxy) ethyl acrylate-*co*-7-(2-methacryloyloxyethoxy)-4-methylcoumarin) (PEEC) acrylic IOL materials were synthesized. The antiproliferative drug 5-fluorouracil (5-FU) could be chemically grafted to the PEEC IOL materials easily via a light induced [2 + 2] cycloaddition reaction with the coumarin group, getting drug-loaded IOL (PEEC@5-FU IOL). The PEEC@5-FU IOL exhibited excellent optical and mechanical properties and biocompatibility. More importantly, the loaded 5-FU could be easily controlled from release by light irradiation via photo-dissociation of the cyclobutane ring that was obtained by the [2 + 2] cycloaddition reaction of 5-FU and coumarin. The in vitro and in vivo experiments demonstrated that such photo-controllable drug release IOL could effectively prevent PCO after implantation in a safe way.

1. Introduction

Cataract is the leading cause of blindness and vision impairment worldwide, posing a significant threat to human vision and quality of life.[1–3] The effective clinical treatment is phacoemulsification combined with intraocular lens (IOL) implantation.[4] However, postoperative complications such as posterior capsule opacification (PCO) can occur months or even years after surgery, leading to visual impairment.[5,6] The incidence of PCO is reported to be 20–40% in adults and almost 100% in infants and children.[7,8] Nd:YAG laser capsulotomy is used as the clinically effective treatment for PCO.[9]] Yet it brings with it other complications, including retinal detachment, retinal tears, IOL pitting or fracture, uveitis, and transient intraocular pressure (IOP) increase, in addition to resulting in financial and psychological burdens.[10–12] Therefore, it remains a major research priority to explore the prevention of PCO in this field.

Many strategies for PCO prevention have been developed, including surgical technique improvement, IOL design amelioration, and IOL material modification.[13,14] As the pathogenesis of PCO is due to opacification resulting from the adhesion, proliferation, and migration of LECs in the posterior capsule (PC) and IOL after cataract operation,[15–17] some researchers have developed antiadhesive IOL to prevent the adhesion of LECs in previous studies.[14,18,19] Currently, the construction of drug-loaded coating on IOL to inhibit cell proliferation via surface modification has attracted wide attention.[20–22] Normal drug eluting IOLs may release the drugs quickly in the early stage after implantation, so uncontrolled drug release may potentially cause unexpected safety issues on surrounding tissues due to the burst release.[13,23] What is more, surface modification requires a complex process, which limits its applicability. In contrast, bulk modification is a more stable, effective and simple method for preparing IOLs.[14] Therefore, controllable drug release bulk IOL materials via stimulus responsiveness are in great demand. In anticipation, we want to get the drug out when the onset of PCO development is observed to achieve the inhibition of PCO occurrence.

Light is a clean, safe and effective stimulus. Compared to other

* Corresponding author.
E-mail address: linqk@wmu.edu.cn (Q. Lin).

https://doi.org/10.1016/j.jconrel.2024.01.007
Received 6 August 2023; Received in revised form 2 January 2024; Accepted 3 January 2024
Available online 11 January 2024

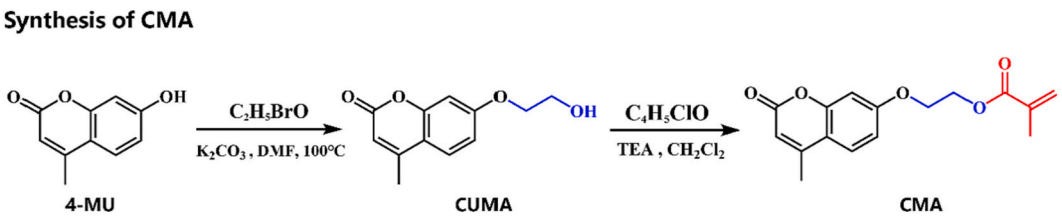

Scheme 2. Synthesis of CMA.

response stimuli, the light response process can be easily controlled by adjusting the wavelength, intensity and duration of light exposure. Currently, there has been extensive research on the application of photo-responsive drug delivery systems in the field of biomedicine.[24–27] Moreover, light can easily pass through the eye compared to other tissues and organs. In ophthalmic clinical therapy, the use of laser technology is common, such as in laser trabeculoplasty, UV riboflavin crosslinking therapy for keratoconus, femtosecond laser in refractive surgery, and photodynamic therapy.[28–31] In conclusion, a photo-controlled drug release system has great application value in ophthalmology and is of great significance for on-demand drug delivery.

Coumarin is a typical photo-responsive molecule, which can undergo a reversible [2 + 2] cycloaddition reaction under UV irradiation.[32–34] 5-Fluorouracil (5-FU) is a pyrimidine analogue, belongs to a class of antimetabolic drugs, and is mainly used in the treatment of tumors.[35–37] 5-FU has also been used to inhibit cell proliferation in ophthalmology.[38,39] Recently, reversible photodimerization and photolysis between coumarin and 5-FU have been reported as a means of photo-controlled release of 5-FU.[40–43] In our previous study, the polymer P (EGPEMA-*co*-EA) (PEE) was designed and synthesized as antifouling IOL material application.[14] In the present investigation, a coumarin derivative, 7-(2-methacryloyloxyethoxy)-4-methylcoumarin (CMA), was introduced into PEE copolymer, resulting in the terpolymer ploy (EGPEMA-*co*-EA-*co*-CMA) (PEEC). Thus, a coumarin contained bulk IOL material was prepared. Under light irradiation at 365 nm, coumarin and 5-FU undergo [2 + 2] cycloaddition reaction, and the drug can be chemically grafted in the material. More importantly, it can be released from the material on demand under light irradiation at 254 nm. It is expected that the material can effectively inhibit PCO after intraocular implantation (See Scheme 1).

2. Experimental

2.1. Materials

4-Methylumbelliferone (4-MU), 2-bromoethanol, potassium carbonate (K_2CO_3), hydrochloric acid (HCl), ethanol, N, N–dimethylformamide (DMF), triethylamine (TEA), and methacryloyl chloride were purchased from Aldrich. Dichloromethane (CH_2Cl_2), 5-FU, EGPEMA, 2-(2-ethoxyethoxy) ethyl acrylate (EA), and 2, 2′-azobis (2-methylpropionitrile) (AIBN) were purchased from Aladdin. Commercial hydrophobic acrylate foldable IOLs were bought from Suzhou 66 Vision Tech Co., Ltd. (66VTs, FV-60 A, the diameter of the optical region was 6 mm). Cell culture medium DMEM/F12 (1:1), fetal bovine serum (FBS), trypsin, and penicillin-streptomycin were purchased from Gibco. Phosphate-buffered saline (PBS) was purchased from Boster Biotechnology. Cell counter kit-8 (CCK-8), Calcein/PI cell viability/cytotoxicity assay kit and Hoechst 33342 staining solution for live cells were obtained from Beyotime Biotechnology. All the eye drops used on animals after the operation were purchased from the Eye Hospital of Wenzhou Medical University.

2.2. Synthesis and preparation

The synthesis route for CMA involved two steps (Scheme 2). To synthesize the precursor, 7-(2-hydroxyethoxy)-4-methylcoumarin (CUMA), the following steps were taken: 4-MU (5.3 g, 30.0 mmol) and K_2CO_3 (8.376 g, 60.0 mmol) were mixed in anhydrous DMF (100 mL) and heated to 100 °C under N_2 protection. Then, 2-bromoethanol (3.2 mL, 45 mmol) was added dropwise. The reaction was refluxed for 20 h. After the reaction, the mixture was cooled to room temperature, and 100 mL of 10% hydrochloric acid was added into it slowly. The potassium carbonate completely dissolved, resulting in an exothermic reaction and cooling to room temperature. Next, 1 l of ultrapure water was added to the mixture and stirred to remove potassium chloride (KCl). The resulting solid was recrystallized with 70 mL of ultrapure water and 50 mL of ethanol. The mixture was cooled naturally to room temperature and stored overnight at 0 °C. Afterward, the solution was filtered and the solid was washed in 500 mL of ultrapure water. The solid was then dried in vacuum at 45 °C for 12 h. The resulting product (CUMA) was obtained as a white solid (5 g, 75.8% yield) and was stored in the dark until required.

To synthesize CMA, CUMA (5.0 g, 22.7 mmol) and TEA (5.0 g, 49.1 mmol) were dissolved in CH_2Cl_2 (70 mL). Methacryloyl chloride (5.0 g, 47.8 mmol) was added dropwise to the stirred solution at 0 °C. After being allowed to warm to room temperature, the solution was stirred overnight. The mixture was then filtered and the filtrate was extracted twice with 100 mL 5% $NaHCO_3$ and twice with ultrapure water. The product was concentrated using rotary evaporation. The crude product was purified by recrystallization from ethanol to obtain CMA. The resulting white solid (2.85 g, 43.7% yield) was stored in the dark until required.

To synthesize PEEC copolymer, EGPEMA (2.08 g, 10.09 mmol), EA (1.25 g, 6.63 mmol), CMA (0.253 g, 0.87 mmol), and AIBN (35.8 mg,

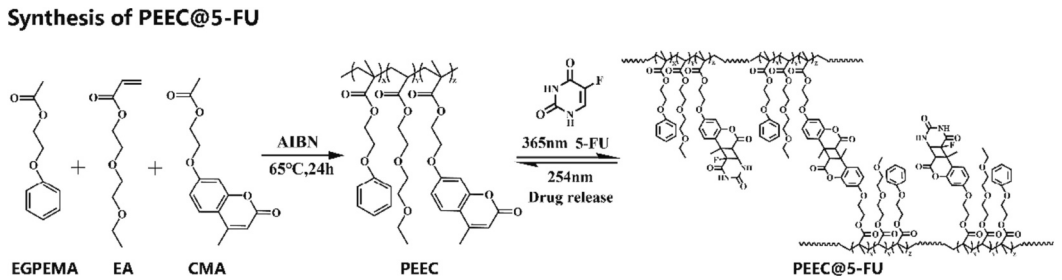

Scheme 3. Synthetic route for PEEC@5-FU.

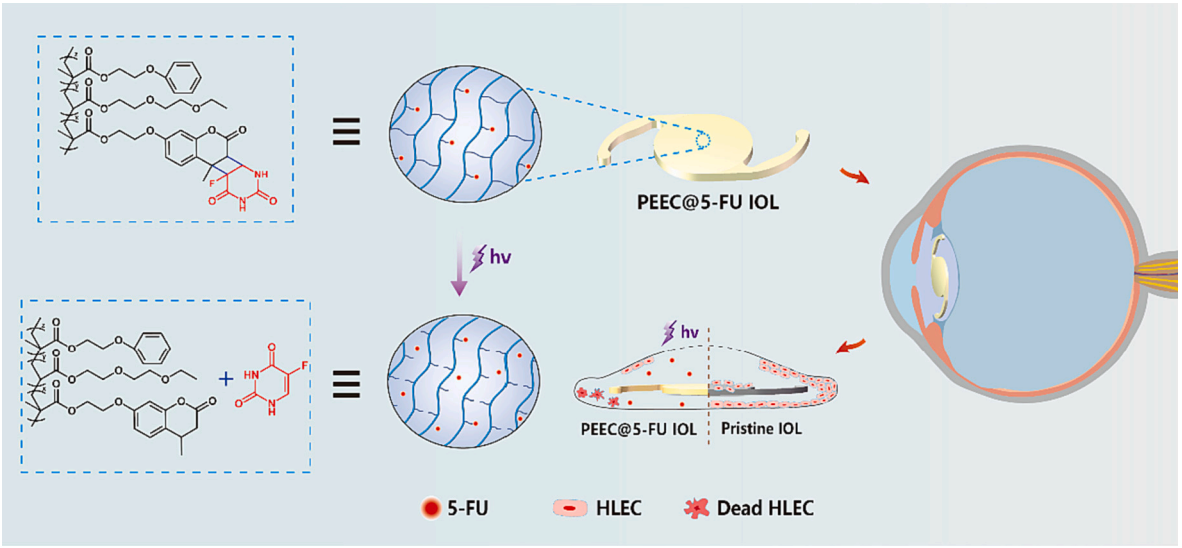

Scheme 1. Schematic diagram for the photo-responsive drug release process of PEEC and the prevention of postoperative capsule opacity through photo-responsive control after implantation of IOL materials.

0.23 mmol) were pretreated with an inhibitor remover and dissolved in 18 mL of DMF in a 25 mL round-bottom flask. The reaction mixture was stirred magnetically at 65 °C for 24 h under N_2 protection. The reaction mixture precipitates in ethanol, and purified PEEC was obtained by dissolution/precipitation cycling. The obtained PEEC was dissolved in DMF, and 5-FU was added to the solution. The resulting solid was sonicated to dissolve it completely and then subjected to 2 h of light irradiation at 365 nm. The solution was then vacuum concentrated to obtain the solid PEEC@5-FU (Scheme 3).

The PEEC copolymer was used to prepare IOL materials. To promote the crystallization process, the copolymer synthesis was changed to bulk polymerization, following these specific steps: First, EGPEMA (2.348 g, 11.4 mmol) and EA (1.431 g, 7.6 mmol) were pretreated with an inhibitor remover and mixed in a molar ratio of 6:4. Then, CMA (0.288 g, 1 mmol) and the initiator (AIBN, 0.02 g) were added sequentially, and magnetically stirred for 30 min to mix evenly. Next, the solution was bubbled with N_2 for 30 min to remove most of the O_2. In order to dissolve the CMA completely, the mixed solution was heated in a water bath at 60 °C. The mixed solution was then injected into cuboid molds (75.6 mm × 25.4 mm × 0.5 mm), sealed, and placed in an oven, allowing for polymerization at 65 °C for 24 h. After polymerization, the materials were placed in alcohol and ultrapure water for ultrasonic cleaning to remove any unreacted monomers.

Afterward, the resulting PEEC IOL was soaked in 5-FU aqueous solution (PEEC IOL/5-FU in a 1:100 M ratio) at 60 °C for 4 days and irradiated with 365 nm light for 2 h. Hence, the [2 + 2] cycloaddition reaction between coumarin and 5-FU enabled the conjugation of 5-FU onto coumarin residue in PEEC IOL. Then, the material was immersed in ultrapure water to remove free 5-FU, and a hydrophobic photo-controlled release IOL material (PEEC@5-FU IOL) was finally prepared.

2.3. Characterization process

The obtained CMA、PEEC and PEEC@5-FU were characterized by Proton Nuclear Magnetic Resonance (^{1}H NMR) spectroscopy (Bruker 400 M, in $CDCl_3$). X-ray photoelectron spectroscopy (XPS) and ultraviolet-visible spectrophotometer (UV–Vis) (Shimadzu, Japan) spectroscopy were utilized to confirm the successful drug loading. The water contact angle (WCA) was evaluated by contact angle analyzer (Data Physics Instrument GmbH, OCA20). The optical transmittance of the materials was measured by UV–Vis in the wavelength range of 200–800 nm with air as the reference. The refractive index of the materials was measured three times for each group by Abbe refractometer (NAR-1 T, Atago Co., Ltd). The thickness of standard dumbbell-shaped specimens was 0.5 mm, and the tensile test was carried out three times for each group at the rate of 10 mm/min at 25 °C (CJinan Metis Test Technology, MT2503).

2.4. Photo-responsive drug loading and release

The detection of changes in the absorbance peak at 320 nm using UV–Vis was utilized three times to monitor the rate of drug release under different light intensities. The method for determining the in vitro release amount of the 5-FU was as follows: PEEC@5-FU IOLs were placed into dialysis bags (MWCO 1000), followed by the addition of 5 mL of PBS respectively. The dialysis bags were then placed into 15 mL of PBS release medium. Irradiation (254 nm) was applied as above mentioned and no light irradiation acted as control. The release concentration of 5-FU was monitored at 266 nm using a calibrated 5-FU standard curve prepared in PBS.

The photo-responsive drug loading and release processes were also confirmed by a Quartz Crystal Microbalance with Dissipation Monitoring (QCM-D, QSense Explorer, Sweden, equipped with a window cell chamber).[44,45] The QCM-D is a sensitive sensor technique to measure a trace of mass changes on the surface. The resonance frequency (F) of the crystal depends on the total oscillating mass, including water coupled to the oscillation.[44] The F decreases when things are attached to the sensor crystal, and it increases when things detach.[44–46] In detail, the PEEC was dissolved in DMF, coated onto the Q-Sense sensor crystal and dried in the oven at 80 °C for 12 h, and the PEE = -coated crystal was obtained and subsequently fixed onto the chamber for testing. Then, ultrapure water was injected into the chamber for rinsing, followed by 1 mg/mL 5-FU aqueous solution injection. The 365 nm light was then irradiated through the window of the chamber at curve equilibrium to facilitate drug loading, followed by water rinsing for removing free drugs. Finally, the 254 nm light irradiation was irradiated through the window for photo-responsive drug release. In this experiment, we want to illustrate the loading and releasing behaviors of drugs through the increase and decrease of the mass after light exposure.

2.5. In vitro cell culture experiment

The cytotoxicity of IOL material extraction was assessed by cell culture. The leach liquors of PEEC IOL and PEEC@5-FU IOL were

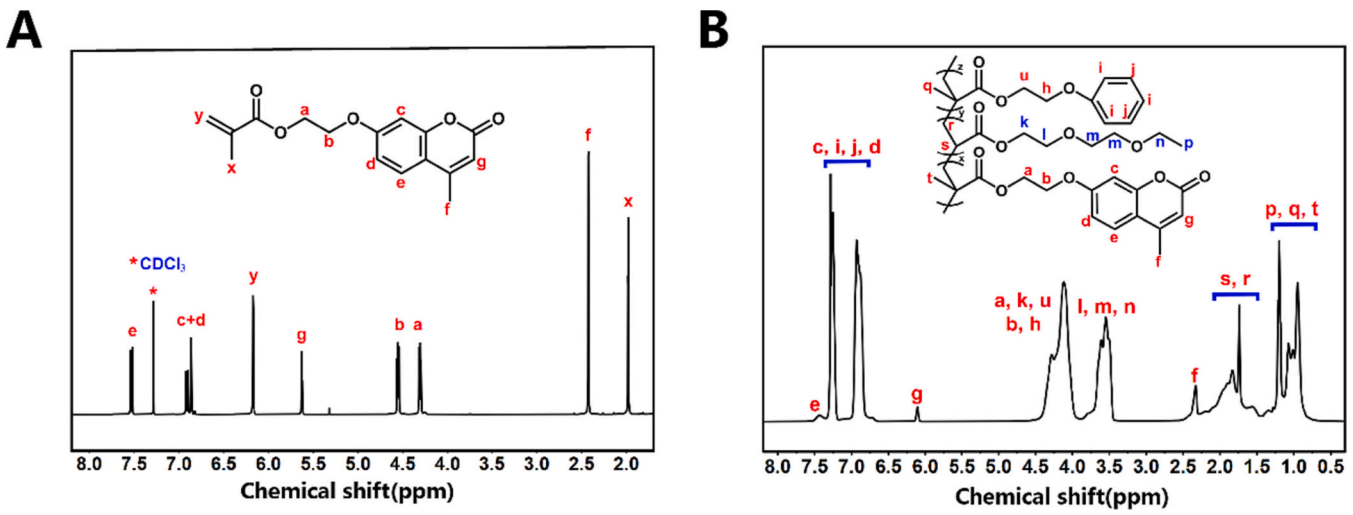

Fig. 1. (**A**) ^{1}H NMR spectrum of the CMA. (**B**) ^{1}H NMR spectrum of the PEEC copolymer.

obtained by soaking in PBS for 30 days. The human lens epithelial cells (HLECs) were cultured in DMEM/F12 (1:1) mixed medium supplemented with 10% FBS and 1% penicillin-streptomycin at 37 °C in a humidified atmosphere with 5% CO_2. Each well was seeded with 5×10^3 cells in 200 μL of complete medium and incubated in an incubator for 24 h. Then, 20 μL of leach liquor was added and incubated for another 24 or 48 h, and cell viability was measured by the CCK-8 method.[13]

5-FU is expected to be released upon 254 nm irradiation and kill any remaining HLECs on the IOL. To verify the antiproliferation effects, the prepared PEEC IOL and PEEC@5-FU IOL were sterilized and placed into a 96-well plate with 100 μL of PBS solution per well. Both PEEC IOL and PEEC@5-FU IOL were irradiated with 254 nm light, while no light irradiation (kept in dark) was carried out as controls. TCPS served as the control. Then, 100 μL of complete medium was added with 5000 cells per well. After 12 or 24 h incubation, the cells were stained with Hoechst 33342 solution and observed by inverted fluorescence microscope (Leica, DMi8). The number of cells was also calculated by ImageJ software (National Institutes of Health, 1.53 t). Dead/alive staining was used to further illustrate the antiproliferative properties. PEEC@5-FU IOL materials were placed into a 96-well plate with 100 μL of PBS solution per well and divided into two groups: one group was irradiated with 254 nm light, while the other was not (kept in dark). The TCPS group was used as a control. Next, 100 μL of culture medium with 5000 cells per well was added and cultured for 24 h. Live/dead staining was then performed and observed by inverted fluorescent microscope.

2.6. Animal experiments

The animal experiments were carried out according to the National Institutes of Health Guidelines for the Care and Use of Laboratory Animals and approved by the experimental animal ethics committee of Wenzhou Medical University. To evaluate the in vivo therapeutic effect of PEEC@5-FU IOL, eight 2-month-old Japanese White-eared rabbits were selected and randomly divided into two groups: the Pristine IOL group and the PEEC@5-FU IOL(hv2) group. Phacoemulsification combined with IOL implantation was performed, and one IOL was implanted in the right eye of each rabbit. The surgery details were the same as in our previous articles.[47,48] Dr. Han led the animal surgery. Light irradiation (254 nm, 4.5 mW/cm^2, 5 min; the illumination distance was around 10 cm) was performed every week after surgery. Levofloxacin, tropicamide, tobramycin-dexamethasone eye drops, and atropine sulfate eye ointment were administered during the first week after the operation. After pupil dilation, slit-lamp microscopy was used to observe the postoperative inflammatory reaction and lens capsular hyperplasia.

Retinal function was evaluated using electroretinography (ERG, Reti-Port21 system, Roland) at the fourth week after surgery to observe the biological safety of the implanted IOLs. At the end of the experiment, the rabbits were euthanized manually. The eyeballs were removed and soaked in the fixative solution for one week. The tissue was separated and dehydrated according to standard procedures. The paraffin sections of the cornea, iris and retina, as well as frozen section of the capsules, were carefully prepared and stained with hematoxylin-eosin (HE). Finally, the obtained sections were observed and photographed to assess the extent of PCO and biocompatibility in vivo.

2.7. Statistical analysis

Three to six parallel samples were set in the experiments, and the results are expressed as mean ± standard deviation. One-way analysis of variance was adopted to compare the statistical difference between two groups. $P < 0.05$ was considered to indicate a significant statistical difference. $P < 0.05$ (*), $P < 0.01$ (**), $P < 0.001$ (***), and $P < 0.0001$ (****) represent significant differences, and $P > 0.05$ represents no significance difference (ns).

3. Results and discussion

3.1. Synthesis of PEEC

^{1}H NMR spectroscopy was used to confirm the successful synthesis of the CMA and PEEC copolymer. As shown in Fig. 1A, the peaks at 6.92–6.85 ppm (protons c, d) and 7.53 ppm (proton e) belonged to the benzene ring. The peak at 2.42 ppm (proton f) was attributed to the methyl group, and the peak at 5.6 ppm (proton g) belonged to the double bond on the pyranone. In Fig. 1B, the peaks ranging from 7.26 to 6.9 ppm (protons i, j) were assigned to the phenyl (-C_6H_5-) group in EGPEMA. The peaks ranging from 3.7 to 3.44 ppm (m, n) corresponded to the (-C_2H_4O-) units in EA, while the peaks at 6.1 (g) and 2.32 (f) were the characteristic peaks of CMA.[49]

3.2. Material properties

3.2.1. Mechanical property

The mechanical tensile test was conducted to determine the elongation at break and elastic modulus of each sample. After 365 nm irradiation (labeled as hv1 for short in the figure presentation), there was a significant increase in the elastic modulus, whereas the elongation at break decreased. Conversely, after 254 nm irradiation (labeled as hv2 for short in the figure presentation), the elastic modulus decreased, while the elongation at break increased (Fig. 2A). In this scenario, when

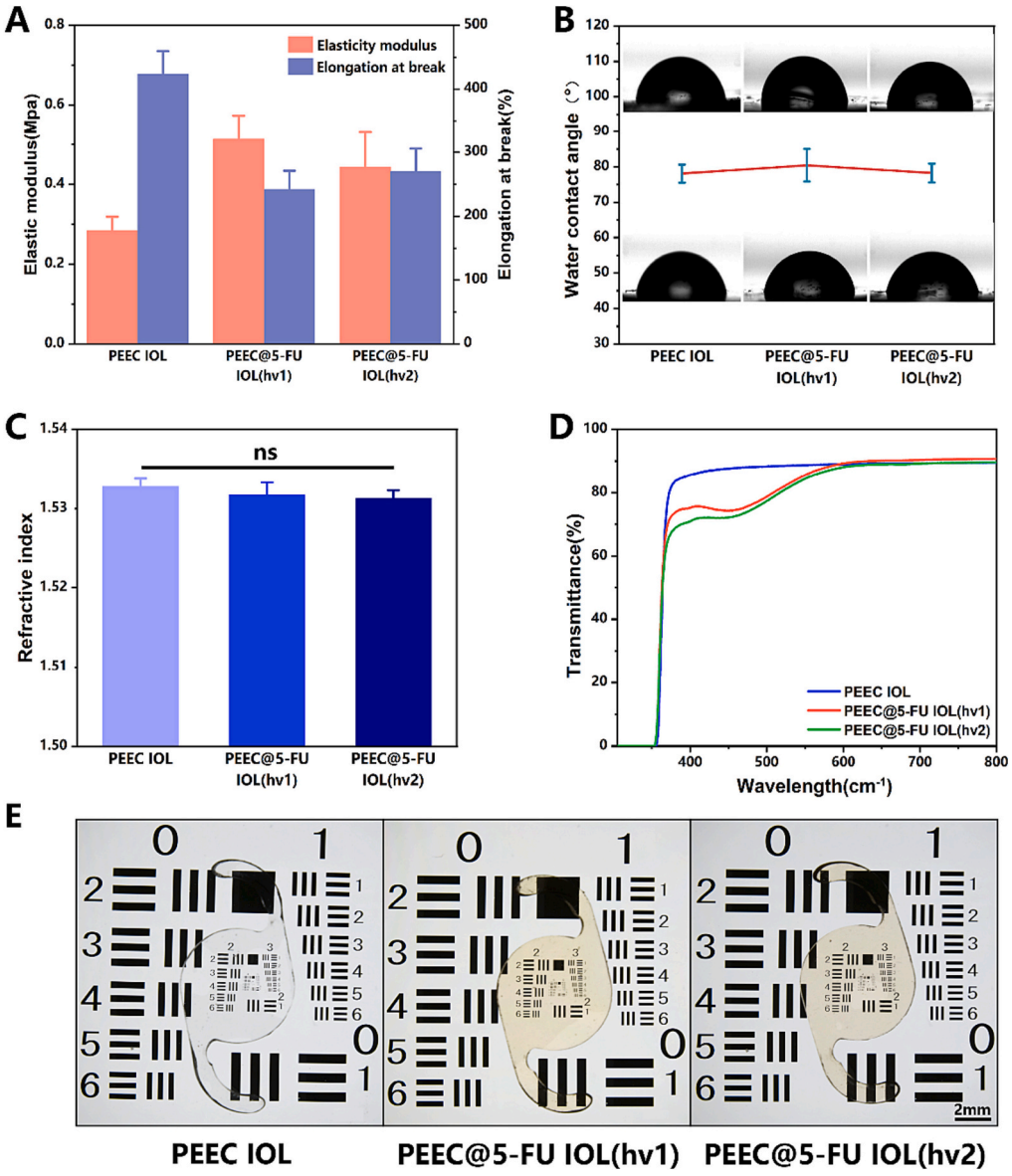

Fig. 2. Physical properties of IOL materials. (PEEC@5-FU IOL(hv1): 5-FU is grafted onto the material when PEEC IOL is exposed to 365 nm light. PEEC@5-FU IOL (hv2): After drug loading, the drug is released when exposed to 254 nm light.) (**A**) Elastic modulus and stretching rate. (**B**) WCA. (**C**) Refractive index. (**D**) Light transmittance. (**E**) Representative image of the IOL placed on an optical resolution plate.

the coumarin groups are exposed to 365 nm light, the [2 + 2] cycloaddition reaction takes place. This reaction results in an increase in the degree of crosslinking and a decrease in molecular mobility. Consequently, the increase in elastic modulus, along with the decrease in elongation at break, occurred due to the increase in the degree of crosslinking resulting from the [2 + 2] cycloaddition reaction induced by 365 nm irradiation. Conversely, after 254 nm irradiation, the degree of crosslinking decreased, leading to an opposite situation.

3.2.2. *Surface wettability*

The surface hydrophilicity of IOL materials plays an important role in preventing LEC adhesion behavior. Thus, the static WCA was used to evaluate the surface wettability. Each group was measured six times. As indicated in Fig. 2B, WCA of PEEC IOL is 78° ± 2.56°. It should be due to the nonpolar side chain of the methyl and phenyl groups on EGPEMA, which decrease the hydrophilicity of the IOL materials. It can also be seen that the WCA values of the three groups are very close to each other, indicating that the loading and release of the drug have no significant effect on the wettability of the material.

3.2.3. *Optical properties*

Optical properties are an essential feature to evaluate IOL. Fig. 2C shows that the refractive index of materials in each group remained nearly constant after irradiation. This revealed that the drug-loading and release process had no effect on the refractive index. It is around 1.53, while standard artificial IOLs need to reach 1.4 or above. The higher the refractive index, the thinner it can be designed, reducing the surgical incision and lowering the risk.[50] As shown in Fig. 2D, the transmittance of the PEEC IOL is about 90% in the visible wavelength range of 390–780 nm. After exposure to light, the transmittance decreased at 400–550 nm, which is the range of blue light. Therefore, the material has a certain absorption capacity to blue light after irradiation, which makes it effective in preventing blue light. In order to evaluate the optical properties of IOL more intuitively, a USAF1951 resolution plate was used to evaluate the resolution of the materials. For the purpose of comparison, the samples were placed above the resolution plate and observed under the stereomicroscope (Fig. 2E). It is not difficult to see that the visual clarities of PEEC@5-FU IOL(hv1) and PEEC@5-FU IOL (hv2) had not changed significantly. The observed color change serves

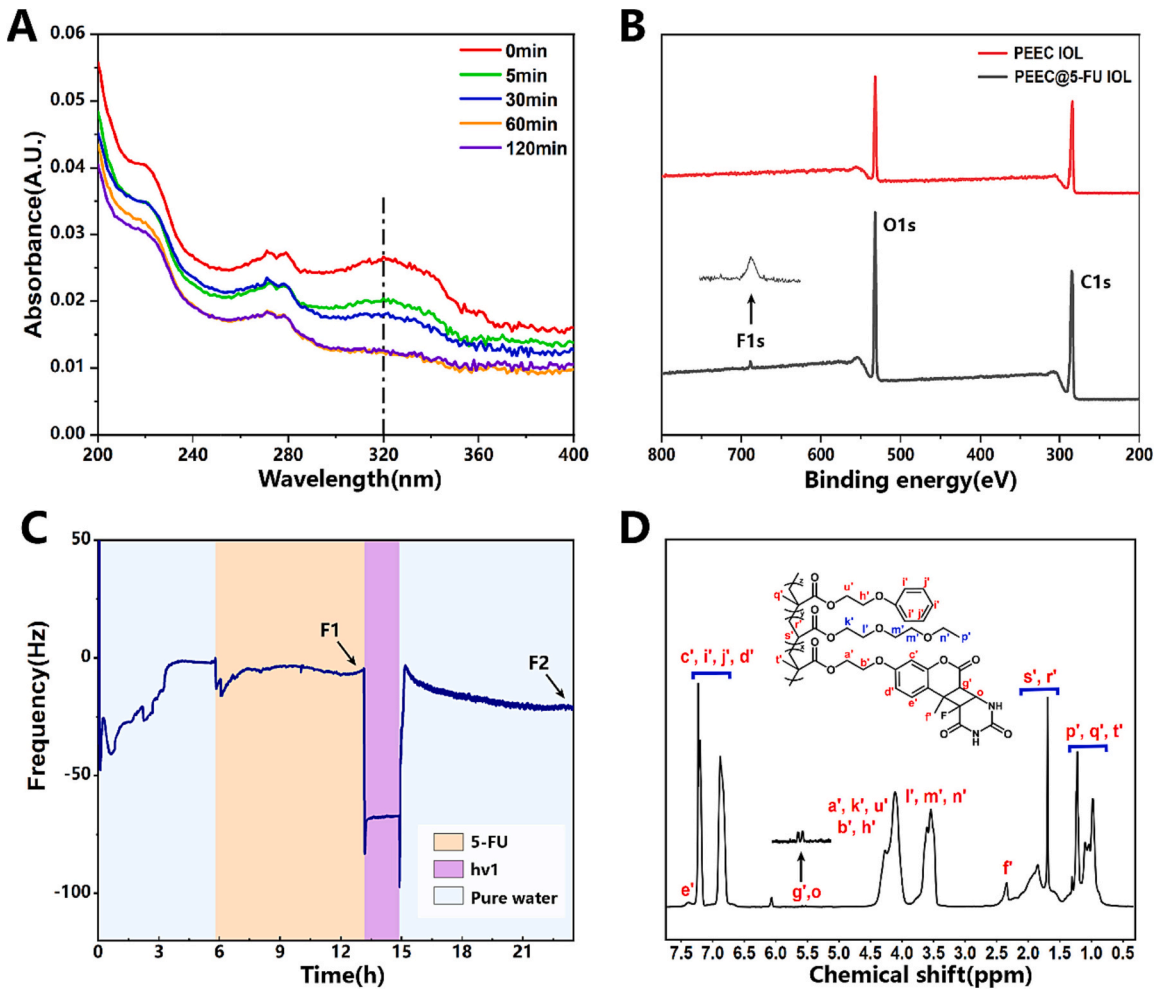

Fig. 3. (**A**) UV–Vis spectra of PEEC IOL treated with 5-FU solution under 365 nm irradiation for different times. (**B**) The XPS spectra of PEEC@5-FU IOL and PEEC IOL. (**C**) Frequency changes of the PEEC IOL material with different treatments in QCM-D measurement. (**D**) ^{1}H NMR spectrum of the PEEC@5-FU copolymer.

as further evidence that 5-FU was successfully loaded into the material, with the depth of color being dependent on the concentration of 5-FU. It can be observed that the image had high clarity, the imaging details were clearly visible, and there were no obvious distortions or noise and no interference factors such as halo or reflection.

3.3. In vitro drug loading

The drug-loading process was analyzed by UV–Vis. The appearance of the coumarin signal peak of 320 nm indicates that the coumarin has been successfully introduced into the IOL material.[51] Fig. 3A shows that the maximum absorbance at 320 nm decreased with the reaction progression. In addition, XPS analysis was performed to examine the elements in the material. Since 5-FU contains fluorine, the appearance of a signal peak for the fluorine element confirmed the successful grafting of 5-FU onto the PEEC material (Fig. 3B). The loading process of drug was also characterized by QCM-D (Fig. 3C).[45] When the 5-FU solution was injected after the water equilibrium, the frequency decreased. This indicates that the drug had penetrated into the material, so the mass had increased. Under 365 nm irradiation, the frequency dropped rapidly, which was partly due to the thermal effect. It can be observed that after exposure and ultrapure water flushing, the frequency was decreasing (F2) when it was compared to the frequency before light irradiation (F1), indicating that 5-FU and PEEC underwent cycloaddition reaction, and the drug was grafted onto the material. The structure of PEEC@5-FU was further analyzed by ^{1}H NMR spectroscopy. As shown in Fig. 3D, compared to the previous results for PEEC (Fig. 1B), the double bond protons of coumarin move to 5.61 ppm, designated as (g'). The double bond of 5-FU shifted to 5.56 ppm, designated as (o). This further confirms the formation of cyclobutane-type bonds and the successful drug loading. Collectively, these results provide evidence that the drug was successfully loaded onto the IOL.

3.4. In vitro drug release

After coumarin is grafted with 5-FU, the characteristic absorbance peak at 320 nm will disappear. However, as 5-FU is gradually released, the characteristic absorption peak will reappear and gradually increase. These characteristics can be used to illustrate drug release behavior. As shown in Fig. 4A, PEEC@5-FU IOL was treated by 254 nm light irradiation with various intensities for different time intervals. It can be seen that with the illumination time increasing, the absorbance at 320 nm gradually increased. Additionally, as the intensity of the irradiation increased, the rise of the absorbance peak gradually speeded up. Based on the above results, it can be concluded that the on-demand release of 5-FU can be effectively achieved by adjusting the irradiation intensity and time. The release process of drugs was also followed by QCM-D (Fig. 4B).[46] Under 254 nm irradiation, the frequency increased, indicating that the drug was released, resulting in a drop in weight. This indicates that the material has favorable photo responsiveness and can respond immediately to light stimulation.

The photo-triggered controlled release profile of 5-FU in PBS solution

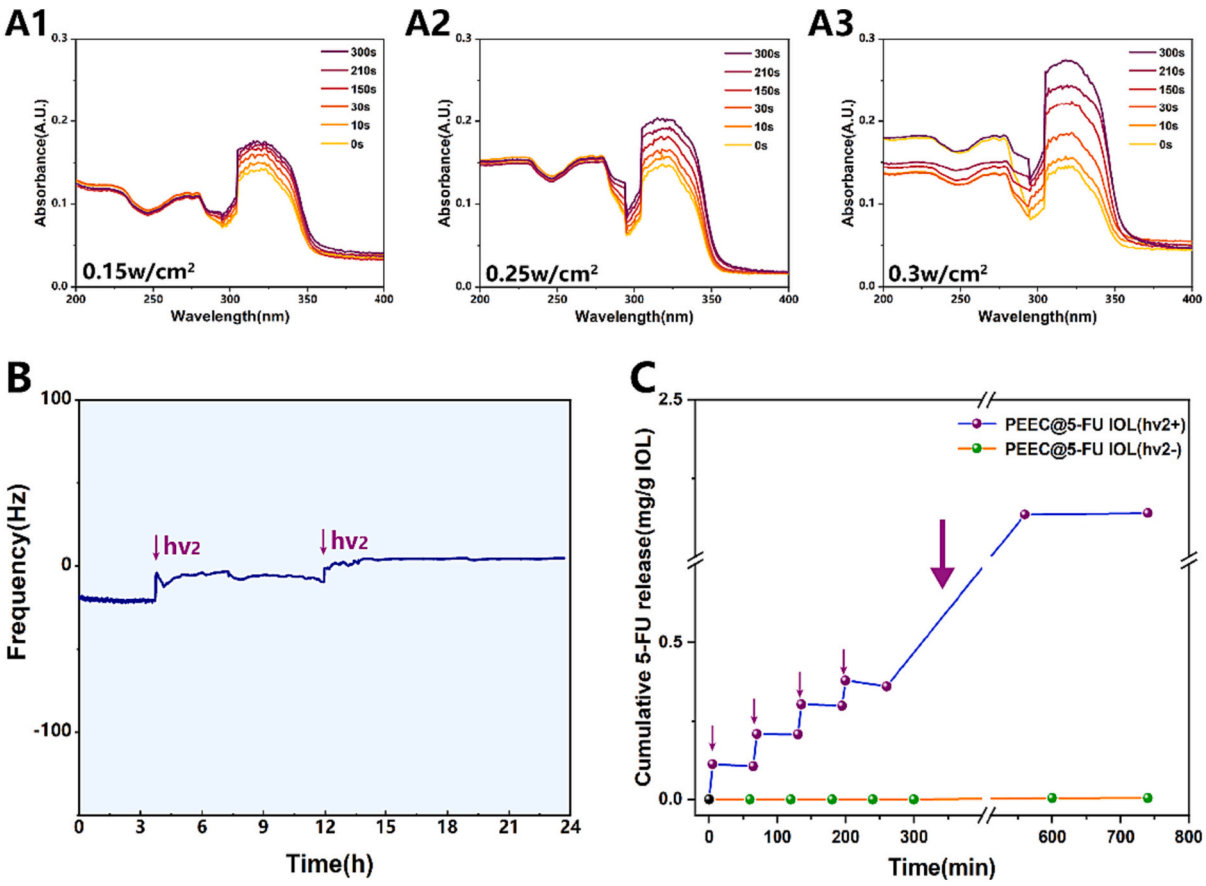

Fig. 4. (**A**) UV–Vis spectra of PEEC@5-FU IOL under 254 nm irradiation for different times at different intensities. (**B**) Frequency changes of the PEEC@5-FU IOL material when triggered by the 254 nm light (hv2) irradiation in QCM-D measurement. (**C**) In vitro 5-FU release profiles from PEEC@5-FU IOL in PBS with or without 254 nm light irradiation (the arrow indicates the time point of the light irradiation).

was studied. The drug release behavior without irradiation was also evaluated to serve as control. The release effect of 5-FU in PBS was evaluated by observing the characteristic absorbance changes of 5-FU molecules. As shown in Fig. 4C, after multiple 5 min, 254 nm irradiations, the absorbance of 5-FU gradually increased, indicating the successful photo-triggered release of 5-FU in PBS. Starting from 260 min, irradiation was done for 5 h to ensure that all drugs were released. By using the 5-FU standard curve in PBS, the in vitro release curve of 5-FU in PBS was obtained and the final amount of drug released from the material was calculated to be around 2.134 mg/g in IOL material. In contrast, the photo-stable cyclobutane linkage cannot be cleaved without irradiation (254 nm). Thus, the drug 5-FU cannot be released. In summary, PEEC@5-FU IOL has excellent photo-controlled drug release ability and can control the amount of drug release by adjusting the light exposure time and intensity.

3.5. *In vitro cell culture experiment*

To investigate whether the released 5-FU has antiproliferation ability under irradiation, the HLECs were stained with Hoechst 33342 and photographed with an inverted fluorescence microscope (Fig. 5A). Statistical analysis was conducted on cell counts after cells were seeded on surfaces of different materials and cultured for a specific period (Fig. 5B). As shown in Fig. 5A and B, there was no significant difference in morphology and quantity of HLECs among 5-FU grafted PEEC IOL materials without 254 nm light exposure (PEEC@5-FU IOL(hv2-)), PEEC IOL materials with 254 nm light exposure (PEEC IOL(hv2+)) and PEEC IOL materials without 254 nm light exposure (PEEC IOL(hv2-)). This showed that irradiation had no obvious effect when no drug was loaded. Compared with TCPS, the number of cells was lower, which was due to the antiadhesion function of the EA component. However, when the 5-FU grafted PEEC IOL materials were exposed to the 254 nm light (PEEC@5-FU IOL(hv2+)), the cell density was significantly further decreased, when compared with the groups of PEEC@5-FU IOL(hv2-), PEEC IOL(hv2+) and PEEC IOL(hv2-), which indicates that the drug could be released only after the material was under irradiation. This finding proves that the material is photo-responsive and has a great antiproliferation ability.

Besides the antiproliferative effect of the designed IOL materials, the biocompatibility is also one of the most critical properties. Therefore, the cell viability of the PEEC@5-FU IOL material extraction on HLECs was evaluated. As shown in Fig. 5C, the cell viabilities of the PEEC IOL and PEEC@5-FU IOL groups were good when compared to that in the control group with PBS. Furthermore, the cell viability of material groups was even slightly higher than that in the PBS after 24 and 48 h of culture, which may be due to the accelerated growth of cells when responding to the mild external stimulation. As shown in Fig. 5D, the cells in the PEEC@5-FU IOL (hv2+) group showed red fluorescence due to death, while cells in the PEEC@5-FU IOL (hv2-) group remained alive and showed green fluorescence, indicating the cytotoxic effect of the drug. Compared with the TCPS group, the PEEC@5-FU IOL material exhibited antiadhesive properties, resulting in a significant reduction in the number of cells adhering to the material.

3.6. *In vivo animal experiment*

The intraocular implantation was performed to verify the in vivo PCO prevention effect of the designed IOL materials. A slit-lamp

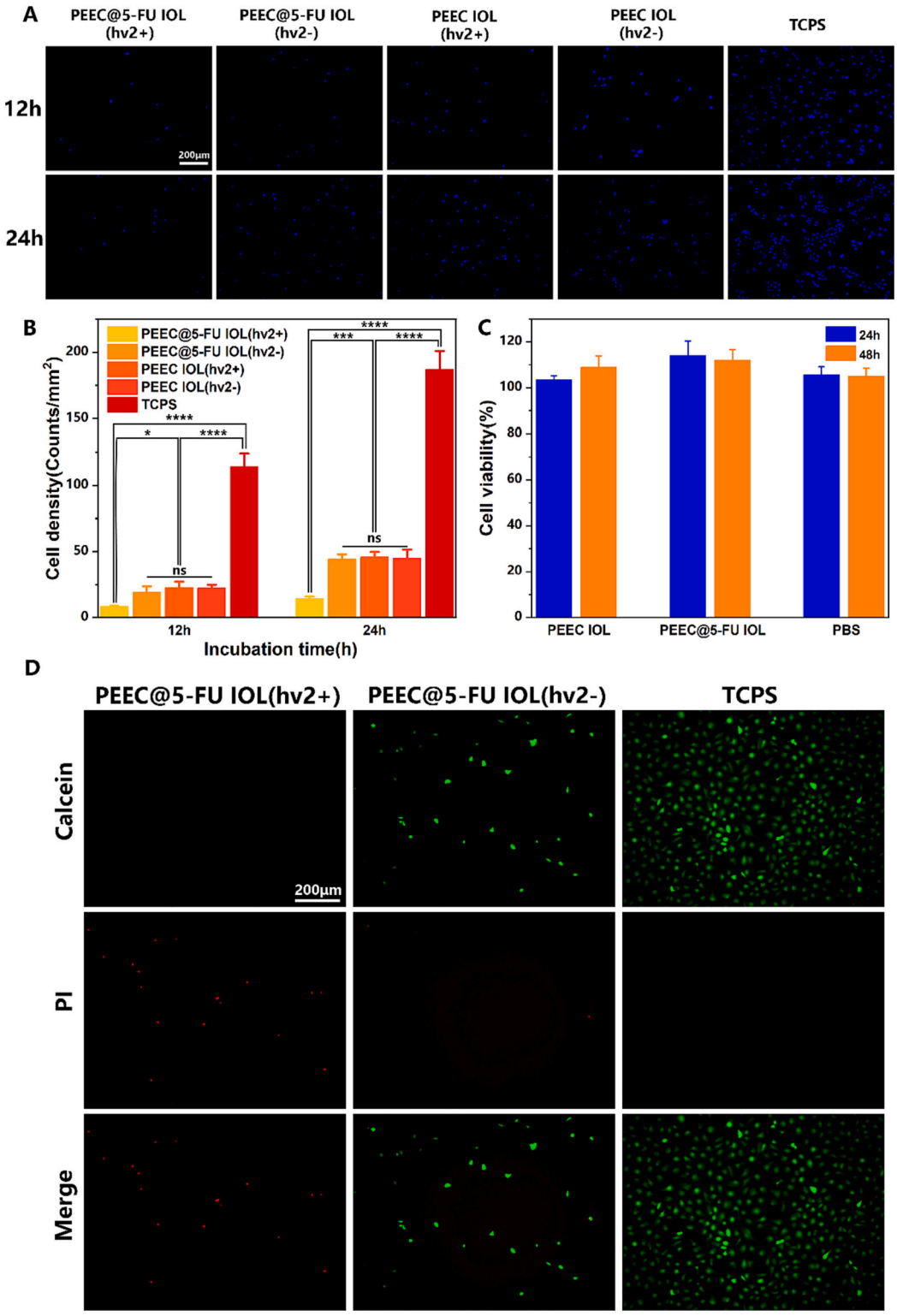

Fig. 5. (**A**) Representative fluorescent images of cells on different material surfaces. (**B**) Cell density on different material surfaces after culturing for 12 or 24 h. (**C**) Cell viability of the PEEC IOL, PEEC@5-FU IOL material extractions and PBS. (**D**) Live/dead staining images of LECs on the surface of PEEC@5-FU IOL after different treatments (hv2 + and -), and TCPS.

microscope was used to observe the short-term inflammation and long-term PCO development. The results indicated that the inflammatory reaction was quite mild in the PEEC@5-FU IOL(hv2) group, with only slight exudation present in the anterior chamber during one week after the implantation (Fig. 6-a1-a3, b1-b3). By the second week, the anterior chamber exudate was absorbed and no significant inflammatory reaction was detected (Fig. 6-a4, b4). Pristine IOL displayed evident cell proliferation during the second week after the operation (Fig. 6-a4), which gradually progressed toward the central optical region (Fig. 6-a5, a6). However, due to the antiproliferation properties of PEEC@5-FU IOL, the peripheral and central regions of the PEEC@5-FU IOL(hv2) group remained transparent (Fig. 6-b4, b5, b6), with only minimal

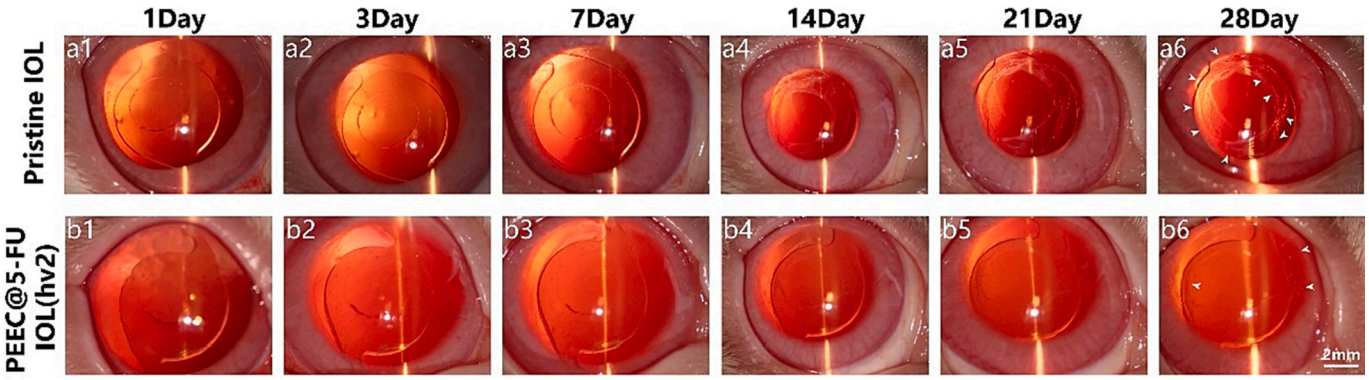

Fig. 6. Representative slit-lamp microscopic images of PEEC@5-FU IOL(hv2) and Pristine IOL implanted eyes at different times after surgery (the white arrow indicates the proliferating cells on the surface of the IOL).

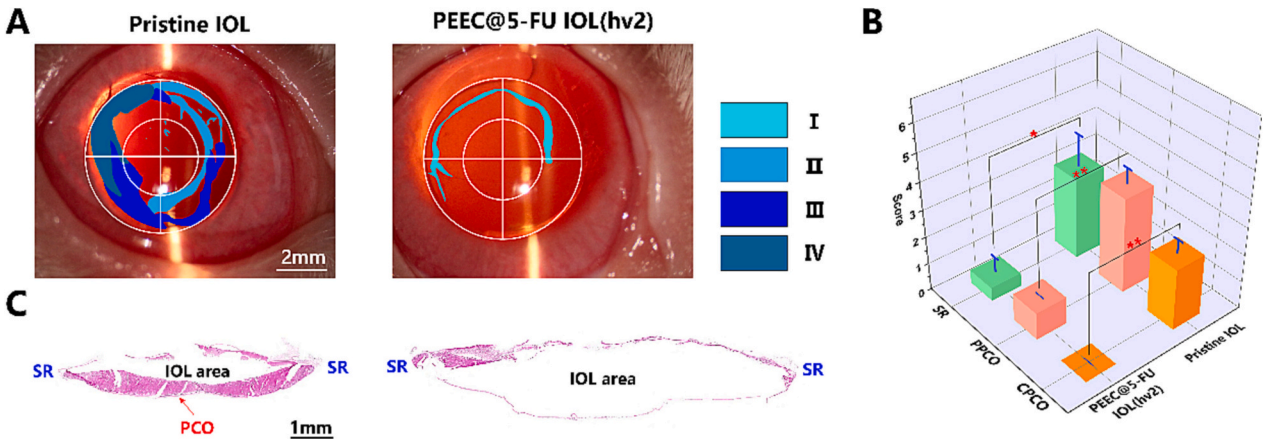

Fig. 7. (**A**) Visualized images of PCO matched with slit-lamp microscopic images. (**B**) PCO clinical evaluation and scoring analysis. Opacification density was graded from 0 to 4 (0 = none, 1 = minimal, 2 = mild, 3 = moderate, 4 = severe). (**C**) Representative HE staining images of capsules of the Pristine IOL group and the PEEC@5-FU IOL(hv2) group.

proliferation observed (Fig. 6-b6).

To evaluate the PCO development and the impact on the IOL transparency, PCO was divided into Soemmerring ring (SR), peripheral PCO (PPCO, peripheral zone hyperplasia of the IOL) and central PCO (CPCO, central zone hyperplasia of the artificial lens). The entire capsule was divided into four quadrants and scored based on the severity of opacity. Fig. 7A shows the visualized images of the PCO severity of the slit-lamp microscopic images of PEEC@5-FU IOL(hv2) and Pristine IOL implanted eyes after 28 days (corresponding to Fig. 6-a6, b6), which directly indicates the heavy PCO degree of the untreated Pristine IOLs. The score results were subjected to statistical analysis. As shown in Fig. 7B, the scores of the Pristine IOL group for all parts were higher than those of the PEEC@5-FU IOL(hv2) group, and the difference was statistically significant. Moreover, the CPCO score of the PEEC@5-FU IOL(hv2) group was 0, while that of the Pristine IOL group was 2.25 ± 0.5. These results indicate the efficient PCO prevention effect of the designed drug controllable release IOLs.

The HE staining of capsule sections was also carried out to further confirm the PCO severity. In the Pristine IOL group, significant SR and more severe tissue hyperplasia in PC were observed (Fig. 7C). However, in the PEEC@5-FU IOL(hv2) group, no significant tissue hyperplasia was observed in PC, and the SR was not prominent. These results suggest that PEEC@5-FU IOL(hv2) can alleviate the severity of PCO and inhibit its occurrence.

The biocompatibility and biosafety of the material were further verified through HE staining of surrounding tissue sections. As shown in Fig. 8A, the staining of cornea, iris, and retinal tissue sections showed that PEEC@5-FU IOL did not cause histomorphology damage or adverse effects on the surrounding tissues. As shown in Fig. 8B, the ERGs of normal eyes (left eye) and surgical eyes (right eye) in the PEEC@5-FU IOL(hv2) implantation group were analyzed. The ERG curves of both left and right eyes were found to be similar in both dark and light adaptation. These results proved that the material possesses favorable biocompatibility and biosafety.

4. Discussion

Although IOL implantation is the standard process of cataract treatment, the postoperative high incidence of the PCO remains the main obstacle for long-term vision recovery.[52] As PCO is caused by the adhesion, proliferation, migration and epithelial-mesenchymal transformation of residual LECs in the lens capsule,[15–17] the drug eluting IOLs loaded with the antiproliferative drugs emerge as an effective way for conquering the PCO after its implantation in recent years.[53] However, concerns over the safety of uncontrolled proliferative drug release have arisen. Therefore, a controlled drug release strategy is needed for safer PCO prevention.[13,43] In this study, the photo-controlled drug release IOL material was designed and prepared via the light induced [2 + 2] cycloaddition and dissociation reaction between coumarin and 5-FU just by employing the coumarin group contained monomer in the PEEC polymer material synthesis, followed by a simple light irradiation process. The prepared PEEC@5-FU materials exhibited excellent optical and mechanical properties and biocompatibility, which indicates that the fabricated PEEC@5-FU materials are feasible for IOL applications.

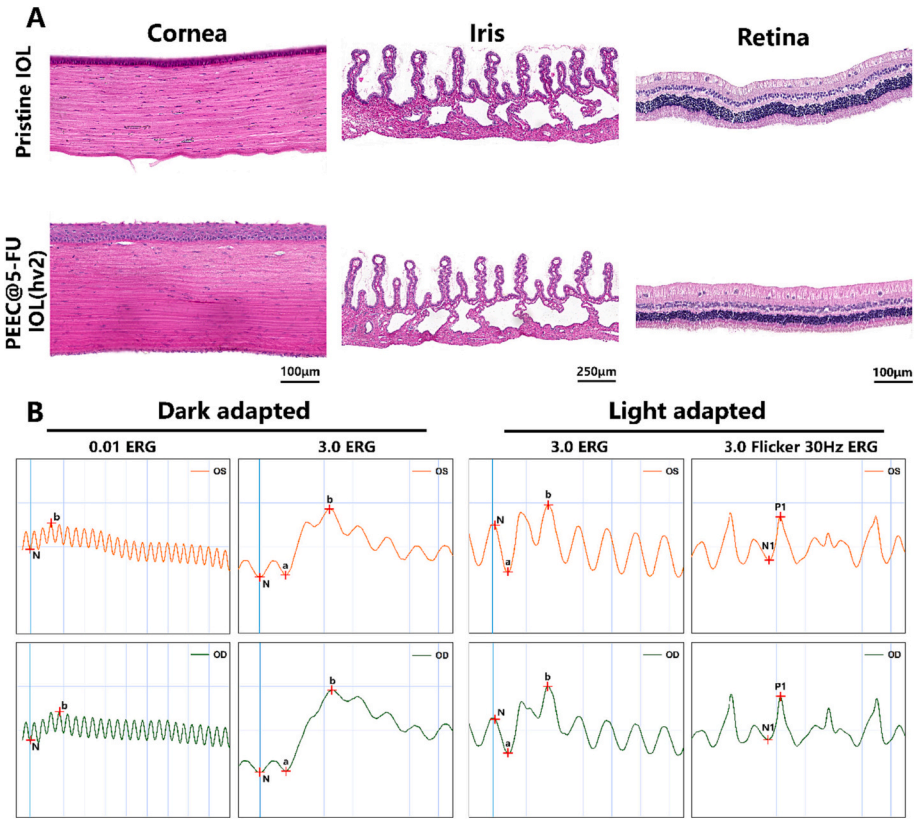

Fig. 8. (**A**) Representative HE staining images of cornea, iris and retina in the Pristine IOL group and the PEEC@5-FU IOL(hv2) group. (**B**) ERG of the operated eye (OD) and normal eye (OS) in the PEEC@5-FU IOL(hv2) group.

Thus, we processed a punching iron mold to process plain IOLs for in vitro or in vivo experiments. As the main purpose of this investigation is to reduce the PCO incidence, we use only one shape of mold design for the IOL laboratory manufacturing. The shape is the same with the obtained commercial IOLs (6 mm diameter of the central optical area with two S-shaped loops, as shown in results of the animal implantation). By using this punching iron mold, the plain IOLs can be easily produced by pressing the mold onto the material sheets, and the production yield for this experimental process is almost 100%. It should be noted that it is just laboratory work and not industrial processing. However, the above in vitro mechanical property investigation results have shown that such PEEC@5-FU materials are suitable for industrial processing.[54–56]

In addition to the physicochemical properties and manufacturing of the IOLs, the photo-controlled drug release profiles of the PEEC@5-FU IOL materials were verified. As mentioned above, PCO has a high incidence (20–40% in adults) of postoperative complication of IOL implantation.[7,8] Although the drug loading onto/into the IOLs can effectively prevent PCO, the uncontrolled drug elution brings with it biosafety concerns. As a result, the photo-controlled drug releasing PEEC@5-FU IOL design provides a precise and safer approach for PCO prevention and control. To be more specific, the material's inherent antiadhesive properties first reduce the probability of PCO occurrence.[14] Then, when symptoms of PCO are observed in the postoperative follow-up of the cataract patient, the light irradiation will be done for releasing the drugs to clear the proliferated cells. If no symptom of PCO is found, nothing will be done and the drugs just stay in the IOLs. This approach aligns more closely with practical clinical application scenarios and provides a precision medicine option.

5. Conclusion

In this study, the photo-sensitive polymer PEEC was successfully synthesized by bulk polymerization, and then the antiproliferative drug 5-FU was grafted onto the IOL through a photo crosslinking reaction. After the drug loading, the material property investigations demonstrated that the PEEC@5-FU IOL possesses excellent mechanical, optical and surface properties. In vitro analysis indicated that drug release can be effectively controlled by simply adjusting the intensity and duration of irradiation, and it can effectively inhibit cell proliferation. Moreover, the material maintains excellent cytocompatibility. The in vivo implantation results not only showed the excellent inhibitory effect on PCO, but also confirmed the safety and biocompatibility of the material with surrounding tissues. In summary, the designed bulk IOL material has excellent photo-controlled drug release ability and can control drug release by adjusting light exposure parameters, achieving on-demand drug release. Such photo-controlled drug releasing bulk IOL material provides a new strategy for effective and safer PCO prevention.

Declarations of competing interest.

The authors declare that they have no financial and personal relationships with other people or organizations that could have appeared to influence the work reported in this article.

CRediT authorship contribution statement

Yulin Hu: Writing – original draft, Visualization, Software, Methodology, Investigation, Conceptualization. **Jiahao Wang:** Writing – review & editing, Investigation. **Yueze Hong:** Methodology, Investigation. **Yuemei Han:** Methodology, Investigation. **Lin Liang:** Methodology, Investigation. **Yuexin Yang:** Investigation. **Zhihui Wu:** Investigation. **Quankui Lin:** Writing – review & editing, Supervision, Project administration, Methodology, Funding acquisition, Conceptualization.

Data availability

Data will be made available on request.

Acknowledgments

This work was financially supported by the Zhejiang Provincial Natural Science Foundation [LR23H180001] and the Key Scientific and Technological Innovation Projects in Wenzhou [ZY2021002].

References

[1] Y.-C. Liu, M. Wilkins, T. Kim, B. Malyugin, J.S. Mehta, Cataracts. Lancet 390 (2017) 600–612.
[2] R.R.A. Bourne, et al., Causes of vision loss worldwide, 1990-2010: a systematic analysis, Lancet Glob. Health 1 (2013) E339–E349.
[3] M.V. Cicinelli, J.C. Buchan, M. Nicholson, V. Varadaraj, R.C. Khanna, Cataracts, Lancet 401 (2023) 377–389.
[4] J.C. Lim, M. Caballero Arredondo, A.J. Braakhuis, P.J. Donaldson, Vitamin C and the Lens: new insights into delaying the onset of cataract, Nutrients 12 (2020) 3142.
[5] X. Zhang, et al., Drug-eluting intraocular lens with sustained bromfenac release for conquering posterior capsular opacification, Bioact. Mater. 9 (2022) 343–357.
[6] M. Ying-Yan, et al., NIR-triggered drug delivery system for chemo-photothermal therapy of posterior capsule opacification, J. Control. Release Off. J. Control. Release Soc. 339 (2021) 391–402.
[7] A.R. Vasavada, M.R. Praveen, Posterior capsule opacification after phacoemulsification: annual review, Asia-Pac. J. Ophthalmol. Phila. Pa 3 (2014) 235–240.
[8] P. Sen, et al., Posterior capsule opacification rate after phacoemulsification in pediatric cataract: hydrophilic versus hydrophobic intraocular lenses, J Cataract Refract Surg 45 (2019) 1380–1385.
[9] I. Hecht, et al., Anti-inflammatory medication after cataract surgery and posterior capsular opacification, Am. J. Ophthalmol. 215 (2020) 104–111.
[10] J.D. Wesolosky, M. Tennant, C.J. Rudnisky, Rate of retinal tear and detachment after neodymium:YAG capsulotomy, J Cataract Refract Surg 43 (2017) 923–928.
[11] A. Grzybowski, P. Kanclerz, Does Nd:YAG capsulotomy increase the risk of retinal detachment? Asia-Pac. J. Ophthalmol. Phila. Pa 7 (2018) 339–344.
[12] D.J. Apple, et al., Eradication of posterior capsule opacification: documentation of a marked decrease in Nd:YAG laser posterior capsulotomy rates noted in an analysis of 5416 pseudophakic human eyes obtained postmortem, Ophthalmology 108 (2001) 505–518.
[13] Y. Hong, et al., Design of foldable, responsively drug-eluting polyacrylic intraocular lens bulk materials for prevention of postoperative complications, J. Mater. Chem. B 10 (2022) 8398–8406.
[14] D. Liu, et al., Foldable bulk anti-adhesive Polyacrylic intraocular Lens material design and fabrication for posterior capsule opacification prevention, Biomacromolecules 23 (2022) 1581–1591.
[15] J. Tang, et al., Surface modification of intraocular lenses via photodynamic coating for safe and effective PCO prevention, J. Mater. Chem. B 9 (2021) 1546–1556.
[16] I.M. Wormstone, Y.M. Wormstone, A.J.O. Smith, J.A. Eldred, Posterior capsule opacification: What's in the bag? Prog. Retin. Eye Res. 82 (2021) 100905.
[17] H. Huang, et al., Cascade catalytic platform modified intraocular lens for high-efficient posterior capsule opacification prevention, Chem. Eng. J. 427 (2022) 131553.
[18] Y. Han, et al., Bottom-up fabrication of zwitterionic polymer brushes on intraocular lens for improved biocompatibility, Int. J. Nanomedicine 12 (2017) 127–135.
[19] Q. Lin, et al., Hydrophilic modification of intraocular lens via surface initiated reversible addition-fragmentation chain transfer polymerization for reduced posterior capsular opacification, Colloids Surf. B Biointerfaces 151 (2017) 271–279.
[20] A. Topete, et al., Dual drug delivery from hydrophobic and hydrophilic intraocular lenses: in-vitro and in-vivo studies, J. Control. Release Off. J. Control. Release Soc. 326 (2020) 245–255.
[21] D. Lu, et al., Centrifugally concentric ring-patterned drug-loaded polymeric coating as an intraocular lens surface modification for efficient prevention of posterior capsular opacification, Acta Biomater. 138 (2022) 327–341.
[22] J. Xia, et al., Facile multifunctional IOL surface modification via poly(PEGMA-co-GMA) grafting for posterior capsular opacification inhibition, RSC Adv. 11 (2021) 9840–9848.
[23] Y. Han, et al., Anti-adhesive and Antiproliferative synergistic surface modification of intraocular Lens for reduced posterior capsular opacification, Int. J. Nanomedicine 14 (2019) 9047–9061.
[24] C. Alvarez-Lorenzo, L. Bromberg, A. Concheiro, Light-sensitive intelligent drug delivery systems, Photochem. Photobiol. 85 (2009) 848–860.
[25] I. Koryakina, et al., Optically responsive delivery platforms: from the design considerations to biomedical applications, Nanophotonics 9 (2020) 39–74.
[26] C. Zhang, et al., Thin film nanoarchitectonics of layer-by-layer assembly with reduced graphene oxide on intraocular lens for photothermal therapy of posterior capsular opacification, J. Colloid Interface Sci. 619 (2022) 348–358.
[27] Z. Ye, et al., Two-dimensional ultrathin Ti3C2 MXene nanosheets coated intraocular lens for synergistic photothermal and NIR-controllable rapamycin releasing therapy against posterior capsule opacification, Front. Bioeng. Biotechnol. 10 (2022) 989099.
[28] P. Kim, G.L. Sutton, D.S. Rootman, Applications of the femtosecond laser in corneal refractive surgery, Curr. Opin. Ophthalmol. 22 (2011) 238–244.
[29] J. Xie, et al., Overcoming barriers in photodynamic therapy harnessing nano-formulation strategies, Chem. Soc. Rev. 50 (2021) 9152–9201.
[30] C. Wittig-Silva, et al., A randomized, controlled trial of corneal collagen cross-linking in progressive keratoconus three-year results, Ophthalmology 121 (2014) 812–821.
[31] C. Hutnik, et al., Selective laser Trabeculoplasty versus argon laser Trabeculoplasty in Glaucoma patients treated previously with 360° selective laser Trabeculoplasty: a randomized, single-blind, Equivalence Clinical Trial. Ophthalmology 126 (2019) 223–232.
[32] J.P. Chesterman, T.C. Hughes, B.G. Amsden, Reversibly photo-crosslinkable aliphatic polycarbonates functionalized with coumarin, Eur. Polym. J. 105 (2018) 186–193.
[33] L. Li, J.M. Scheiger, P.A. Levkin, Design and applications of Photoresponsive hydrogels, Adv. Mater. 31 (2019) 1807333.
[34] H.-M. Lin, W.-K. Wang, P.-A. Hsiung, S.-G. Shyu, Light-sensitive intelligent drug delivery systems of coumarin-modified mesoporous bioactive glass, Acta Biomater. 6 (2010) 3256–3263.
[35] S.-R. Guo, et al., In vivo evaluation of 5-fluorouracil-containing self-expandable nitinol stent in rabbits: efficiency in long-term local drug delivery, J. Pharm. Sci. 99 (2010) 3009–3018.
[36] S. Vodenkova, et al., 5-fluorouracil and other fluoropyrimidines in colorectal cancer: past, present and future, Pharmacol. Ther. 206 (2020) 107447.
[37] C. Sethy, C.N. Kundu, 5-fluorouracil (5-FU) resistance and the new strategy to enhance the sensitivity against cancer: implication of DNA repair inhibition, Biomed. Pharmacother. Biomedecine Pharmacother. 137 (2021) 111285.
[38] D.A. Bukhari, S.K. Alessa, S.I. Beheiri, Corneal epithelial hyperplasia after 5-fluorouracil injection, Case Rep. Ophthalmol. 9 (2018) 254–256.
[39] X. Zhao, S. Liu, Y. Han, Y. Wang, Q. Lin, Preparation of 5-fluorouracil loaded chitosan microtube via in situ precipitation for glaucoma drainage device application: in vitro and in vivo investigation, J. Biomater. Sci.-Polym. Ed. 32 (2021) 1849–1864.
[40] C. Sinkel, A. Greiner, S. Agarwal, A polymeric drug depot based on 7-(2'-Methacryloyloxyethoxy)-4-methylcoumarin copolymers for Photoinduced release of 5-fluorouracil designed for the treatment of secondary cataracts, Macromol. Chem. Phys. 211 (2010) 1857–1867.
[41] Q. Jin, F. Mitschang, S. Agarwal, Biocompatible drug delivery system for photo-triggered controlled release of 5-fluorouracil, Biomacromolecules 12 (2011) 3684–3691.
[42] X. Yang, D.-F. Chen, L.-S. Li, X.-J. Zhao, M.-X. Zhao, Mesoporous silica nanoparticles loaded with fluorescent coumarin-5-fluorouracil conjugates as mitochondrial-targeting theranostic probes for tumor cells, Nanotechnology 32 (2021).
[43] J. Xia, et al., Photo-responsive intraocular lens with on demand drug release for posterior capsule opacification prevention and improved biosafety, Chem. Eng. J. 430 (2022) 132716.
[44] D.Y. Aykut, O. Yolacan, H. Deligoz, pH stimuli drug loading/release platforms from LbL single/blend films: QCM-D and in-vitro studies, Colloids Surf. A Physicochem. Eng. Asp. 602 (2020) 125113.
[45] H. Deligöz, B. Tieke, QCM-D study of layer-by-layer assembly of polyelectrolyte blend films and their drug loading-release behavior, Colloids Surf. A Physicochem. Eng. Asp. 441 (2014) 725–736.
[46] R.T. Guntnur, N. Muzzio, M. Morales, G. Romero, Phase transition characterization of poly(oligo(ethylene glycol)methyl ether methacrylate) brushes using the quartz crystal microbalance with dissipation, Soft Matter 17 (2021) 2530–2538.
[47] J. Wang, et al., Non-viral gene coating modified IOL delivering PDGFR-α shRNA interferes with the fibrogenic process to prevent posterior capsular opacification, Regen. Biomater. 10 (2023) rbad020.
[48] Y. Han, et al., Drug eluting intraocular Lens surface modification for PCO prevention, Colloid Interface Sci. Commun. 24 (2018) 40–44.
[49] D. Lu, et al., Triply responsive coumarin-based microgels with remarkably large photo-switchable swelling, Polym. Chem. 10 (2019) 2516–2526.
[50] T. Kohnen, D.D. Koch, Experimental and clinical evaluation of incision size and shape following forceps and injector implantation of a three-piece high-refractive-index silicone intraocular lens, Graefes Arch. Clin. Exp. Ophthalmol. Albrecht Von Graefes Arch. Klin. Exp. Ophthalmol. 236 (1998) 922–928.
[51] J. Jiang, B. Qi, M. Lepage, Y. Zhao, Polymer micelles stabilization on demand through reversible photo-cross-linking, Macromolecules 40 (2007) 790–792.
[52] J. Emery, Capsular opacification after cataract surgery: Curr, Opin. Ophthalmol. 10 (1999) 73–80.
[53] R.-P. Zhang, Z.-G. Xie, Research Progress of drug prophylaxis for Lens capsule opacification after cataract surgery, J. Ophthalmol. 2020 (2020) 1–9.
[54] A.I. Grabchenko, N.V. Verezub, S.N. Lavrynenko, M. Horvath, A.G. Mamalis, Precision cutting of optical polymer components for bioengineering applications, J. Mater. Process. Technol. 97 (2000) 126–131.
[55] K.Q. Xiao, L.C. Zhang, The role of viscous deformation in the machining of polymers, Int. J. Mech. Sci. 44 (2002) 2317–2336.
[56] A.G. Mamalis, S.N. Lavrynenko, On the precision single-point diamond machining of polymeric materials, J. Mater. Process. Technol. 181 (2007) 203–205.